

# HIGH-RESOLUTION NEUTRON POWDER DIFFRACTION STUDY OF ICE I<sub>c</sub>

W. Kuhs, D. Bliss, J. Finney

► **To cite this version:**

W. Kuhs, D. Bliss, J. Finney. HIGH-RESOLUTION NEUTRON POWDER DIFFRACTION STUDY OF ICE I<sub>c</sub>. Journal de Physique Colloques, 1987, 48 (C1), pp.C1-631-C1-636. 10.1051/jphyscol:1987187 . jpa-00226453

**HAL Id: jpa-00226453**

**<https://hal.archives-ouvertes.fr/jpa-00226453>**

Submitted on 1 Jan 1987

**HAL** is a multi-disciplinary open access archive for the deposit and dissemination of scientific research documents, whether they are published or not. The documents may come from teaching and research institutions in France or abroad, or from public or private research centers.

L'archive ouverte pluridisciplinaire **HAL**, est destinée au dépôt et à la diffusion de documents scientifiques de niveau recherche, publiés ou non, émanant des établissements d'enseignement et de recherche français ou étrangers, des laboratoires publics ou privés.

HIGH-RESOLUTION NEUTRON POWDER DIFFRACTION STUDY OF ICE I<sub>c</sub>

W.F. KUHS, D.V. BLISS\* and J.L. FINNEY\*

*Institut Laue-Langevin, 156 X, F-38042 Grenoble Cedex, France**\*Birkbeck College, Department of Crystallography, Malet Street, GB-London WC1E 7HX, Great-Britain*

**Résumé** - La glace cubique I<sub>c</sub> deutérée a été étudiée par diffraction de neutrons haute résolution. La structure fine du groupe d'espace Fd3m a été examinée. Les atomes d'hydrogène sont totalement désordonnés et les distances interatomiques sont identiques à celles de la glace I<sub>h</sub>. Bien que l'apparence générale du diagramme de poudre soit cubique, plusieurs anomalies ont été observées. Les effets de taille des particules sont importants et à partir de l'élargissement du pic, une taille moyenne des particules de 160 (30) Å a été calculée. Quelques pics de Bragg montrent un élargissement supplémentaire ou une dissymétrie du côté des faibles angles indiquant l'existence de fautes d'empilement. La présence enfin d'un pic de Bragg non cubique qui a été indexé 100 dans le réseau de la glace I<sub>h</sub> est expliqué en terme de séquence hexagonale dans l'empilement.

**Abstract** - High-resolution neutron powder diffraction data on deuterated cubic ice (ice I<sub>c</sub>) prepared by transforming recovered ice II have been obtained. Structure refinements in the cubic spacegroup Fd3m were performed. The hydrogen atoms are fully disordered and the interatomic distances are found to be identical with those in ice I<sub>h</sub>. Although the general appearance of the powder pattern is cubic, several anomalies have been observed. Particle size effects are important and from the peak broadening a mean particle size of 160(30) Å was calculated. Some Bragg peaks show additional broadening or distinct skewness on the high- or low-angle side indicating the existence of deformation faults in the stacking sequence. The presence of at least one non-cubic Bragg peak, which can be indexed as 100 in the lattice of ice I<sub>h</sub>, is explained in terms of hexagonal sequences in the stacking.

**Introduction**

The existence of a second crystalline ambient pressure modification of the water substance besides hexagonal ice (ice I<sub>h</sub>) is well established. On crystallographic evidence it was named cubic ice (ice I<sub>c</sub>) by König<sup>1</sup>, although it had been observed<sup>2</sup> as a new phase earlier on by Barendrecht<sup>2</sup>, Dewar<sup>3</sup>, Burton and Oliver<sup>4</sup> and McFarlan<sup>5</sup>. A great deal of work has been done since König's<sup>1</sup> electron diffraction study on cubic ice, but one is still far from a full understanding of its structure and properties and even its stability range.

There are several ways of preparing ice I<sub>c</sub>: it can be formed by low-temperature deposition of water vapour in a range between 130 and 150 K<sup>e.g. 1,6</sup>, by transformation on heating of vapour-deposited amorphous ice<sup>e.g. 7</sup>, by transformation on heating of various recovered high-pressure ices<sup>e.g. 8,9,10</sup> or by rapid cooling of aqueous solutions<sup>e.g. 11,12</sup>. Once formed, it is stable from 0°K to approximately 200 K, where it begins to transform into ice I<sub>h</sub>. This transfor-

mation is slow and apparently depends to some extent on the sample history. Transformation temperatures as low as 153 K have been observed<sup>8</sup>, which indicates that ice Ic is probably always metastable with respect to ice Ih. For a more detailed discussion of ice Ic preparation and its transformation behaviour we refer to the literature<sup>13</sup>. The heat of transformation for the ice Ic → ice Ih transition has been measured repeatedly<sup>14,15,16</sup>. The heat evolved was found to be very small ( $< 20 \text{ J mol}^{-1}$ ). This is not really surprising since the hexagonal arrangement of the oxygen atoms in ice Ih is energetically very similar to the presumed cubic arrangement in ice Ic. Indeed the nearest neighbour situation as well as the number of next-nearest neighbours are identical in both forms as, consequently, are the averaged dipole moments and the Coulombic interaction energies<sup>17</sup>. Moreover the calculated density<sup>10</sup>, the librational and vibrational bands<sup>18</sup> and the nuclear magnetic resonance<sup>19</sup> are found to be the same within the experimental error. Only the translational bands show a slight difference<sup>20</sup>, which is expected from the different number of acoustic branches according to the change in symmetry. However, the two forms are distinct in terms of their three-dimensional structure and diffraction seems to be the appropriate tool to quantify similarities and differences in their structures, which ultimately may lead to a better understanding of their relative stabilities.

A series of structural investigations has been performed since König's<sup>1</sup> first analysis. Ice Ic has been studied by electron diffraction<sup>21,22</sup>, X-ray<sup>7,20,23</sup> and neutron diffraction<sup>10</sup>. It has been repeatedly observed that the powder pattern was not a clean cubic one but contained some extra lines, which were mainly attributed<sup>7,10,23</sup> to the constant presence of ice Ih for all the preparation procedures. Bertie & Jacobs<sup>20</sup> however suggested that the extra features may not be due to ice Ih impurity, but the quality of their data did not allow them to pursue this point. Particle size broadening has been found in several studies with mean grain sizes between 130 Å<sup>10</sup> and 400 Å<sup>7</sup>. A full structure refinement has not been reported, but there is some evidence<sup>10,22</sup> that ice Ic has a disordered hydrogen arrangement very similar to ice Ih. The spacegroup for the idealized cubic structure is  $Fd\bar{3}m$  and a hypothetical ordered form could crystallize in the spacegroups  $I4_1md$  or  $P2_12_12_1$ . A partial or fully ordered hydrogen arrangement for ice Ic has been suggested, based on a difference in the heat capacities of cubic and hexagonal ice. Contrasting with the generally accepted close resemblance of cubic and hexagonal ice<sup>8,9</sup>, this finding still awaits further clarification.

We present here the results of a high-resolution neutron powder diffraction study on the deuterated ice Ic and a preliminary analysis of the powder pattern obtained will be given, whereby special attention will be paid to the anomalies in the pattern.

## Experimental

Cubic ice Ih ( $D_2O$ ) has been obtained by warming ice II recovered at ambient pressure and 77 K. The heating process was not controlled and occurred when the sample was transferred from the helium-pressure cell<sup>26</sup> to the cryostat, which was held at a temperature of 78(1) K. Neutron powder diffraction patterns were recorded on the high-resolution powder diffractometer D1A at the Institut Laue-Langevin, Grenoble, at wavelengths of 1.390, 1.909 and 2.988 Å. The pattern obtained at 1.909 Å is shown in Fig. 1. All peaks in the diffraction pattern were analysed in the usual way by fitting the position, the full-width at half-height (FWHM) and the height of a Gaussian distribution to the observed peak-shape. Integrated intensities were calculated from the obtained peak parameters and corrected for Lorentz effects. A first inspection of the patterns indicated a broadening of the Bragg peaks at higher angles. The broadening specific to the ice Ic sample was obtained by comparing it with the instrumental broadening as established with an ice II sample of comparable size. Structure refinements were performed with the 1.390 Å data using the PROMETHEUS<sup>27</sup> suite of programs modified for the use of integrated powder intensities; due to the irregular broadening of some Bragg peaks the usual profile refinement technique could not be applied.

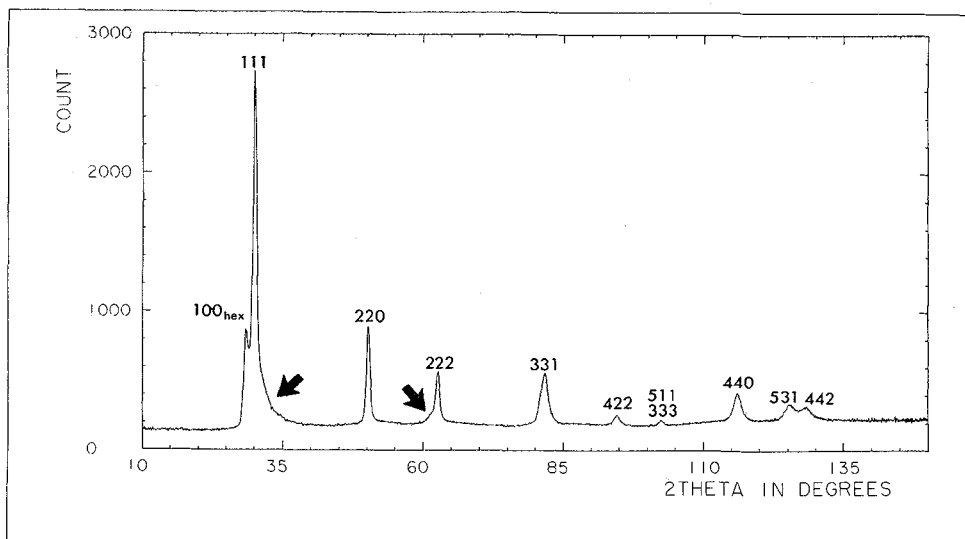


Figure 1 Neutron powder diffraction pattern of heavy ice Ic recorded at 78 K with 1.909 Å neutrons. Note the shoulders on the 111 and 222 reflections (arrows).

**Results**

The powder pattern of ice Ic shows three unusual features: the lines are broadened in a complicated way, some lines have distinct shoulders and at least one reflection cannot be indexed in the presumed cubic lattice. Still, the general appearance of the pattern is clearly cubic as confirmed by the structure refinement. The integrated intensities used in the refinement include all anomalies (shoulders, broadening), which were described - if necessary - by additional Gaussian components overlapping with the main peak. The refinement was done in the spacegroup  $Fd\bar{3}m$  and converged with a weighted R-factor of 0.058. There was - apart from the cubic 111 reflection - no indication of the presence of hexagonal reflections superimposing on the cubic lines. Structure factor calculations in the hypothetical ferroelectrically and antiferroelectrically ordered spacegroups  $I4_1md$  and  $P2_12_12_1$  respectively gave strong disagreement. Table 1 gives the refined structural parameters.

Table 1: The idealized structure\* of ice Ic at 78 K

Atom	Position	Isotropic B
O	$\frac{3}{8} \frac{3}{8} \frac{3}{8}$	1.56(59)
D	xxx with $x = 0.4670(19)$	2.02(64)**

\* Origin at centre of inversion

\*\* Equivalent isotropic B; the root mean-square displacements of the anisotropic thermal motions are 0.093 Å along the OH bond and 0.184 Å perpendicular to the bond direction.

The lattice constant obtained from a least-squares refinement based on five strong peaks of the 1.909 Å run is 6.358(3) Å. With this value and the positional parameters given in Table 1 the following interatomic distances are found:  $r_{OD} = 1.013(14)$  Å,  $r_{O...O} = 2.735(2)$  Å and  $r_{D...D} = 2.287(4)$  Å. Within the limit of error they agree with the corresponding distances in ice Ih. It should be

mentioned that the actual interatomic distances are likely to differ from the quoted values due to unresolved molecular disorder similar to the situation in ice Ih<sup>28,29</sup>, where equilibrium distances  $r_{OD}^e \approx 0.974$  Å and  $r_{O...O} \approx 2.76$  Å have been found. The limited accuracy of the powder data prevents a more detailed analysis of the atomic probability distributions in ice Ic.

The analysis of particle size broadening effects was not entirely straightforward. Some reflections seemed to be more affected than others, in particular the 331 and 533 peaks were much broader than expected for isotropic particles. The hypothesis of anisotropic particle size broadening was considered, but a model consistent with the observed broadening could not be found. Indeed the anomalous broadening of the 331 and 533 peaks can be explained otherwise, as discussed below. The particle size  $L$  was calculated according to the Scherrer formula

$$L = \frac{K \cdot \lambda}{\cos \theta \cdot W'}$$

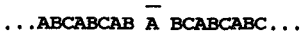
The Scherrer constant for spherical particles ( $K = 1.209$ ) was used;  $\lambda$  is the wavelength and  $\theta$  the scattering angle. The particle size obtained from the 111, 220, 222 and 440 peaks is 160(30) Å. The best internal consistency between the values obtained for different wavelengths was achieved by calculating the half-width  $W'$  originating in the small particle size according to the empirical formula<sup>30</sup>

$$W' = (W_{obs}^2 - W_o^2) / W_{obs}$$

with  $W_{obs}$  the observed full-width at half-height, and  $W_o$  the width calculated from the measured instrumental resolution. The distribution of particle sizes

therefore seems to be neither of a Gaussian ( $W'^2 = (W_{obs}^2 - W_o^2)$ ) nor of a Cauchy type ( $W' = W_{obs} - W_o$ ), but it is located somewhere between the two.

Line broadening and skewness have a variety of origins. The characteristics of the ice Ic pattern however indicate strongly the existence of deformation faults, i.e. stacking faults of the type



which means that the regular packing sequence of a cubic structure is perturbed only at the indicated position. This contrasts with so-called growth-faults, where the whole sequence is mirrored from the faulty plane onwards



The two stacking faults may be distinguished by their powder pattern<sup>31</sup>. In Fig. 2 the reciprocal lattice of a deformation faulted cubic lattice is given .

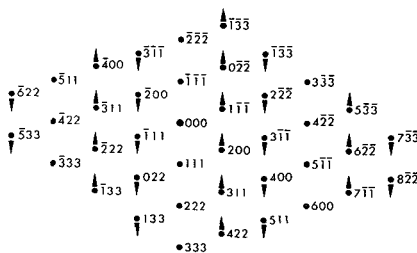


Figure 2 : Section of reciprocal lattice of an ice Ic single crystal with deformation faults. The arrows indicate the shift direction of the broadened intensity maxima. Note that along [111] there is no shift and no broadening. Powder patterns correspond to a superposition of all reciprocal lattice points at a given distance from the origin.

It shows that the shoulder on the 111 reflection is on the high-angle side, while it is on the low-angle side of the 222 reflection. Some other reflections exhibit both a high- and a low-angle component. Most reflections have sharp central features (as seen in the figure for the 111 direction). Indeed, all reflections with indices  $h+k+l = 3n$  are not broadened, which on the other hand means that all equivalent reflections of  $hkl$ 's with two indices equal to  $3n$  and one index unequal to  $3n$  have no sharp component at all (e.g. 400, 800, 331, 533). Thus the anomalous broadening of the 331 and 533 can be understood (the 400 and 800 are very weak reflections and cannot be analysed for their broadening). A quantitative analysis has not been performed; the available formalisms<sup>e.g. 91</sup> are strictly valid only for infinite crystals and random distribution of faults; it is established that the crystallites are very small and it is probable that some clustering of faults occurs as discussed below. The magnitude of the skew components and their position however, indicates that the probability of a deformation fault occurring is of the order of a few percent.

Finally, the first diffraction peak needs some consideration. Its centre is very close to the calculated position of the 100 reflection of ice Ih. A high density of growth faults would result in the appearance of broadened hexagonal peaks. Indeed the 100 peak probably has a shoulder on its high angle side (as indicated by fitting the complex first diffraction peak with overlapping Gaussians), but there is no sign of any reflection of hexagonal ice with  $l \neq 0$ ; thus the probability of the occurrence of growth faults must be small. Hexagonal reflections other than the 100 are not observed (with the possible exception of the 101 peak, which coincides with the high-angle shoulder of the cubic 111 peak). The presence of a strong hexagonal 100 peak may be explained by the occurrence of regular stacking sequences. Most of the other hexagonal reflections of such a polytype are weak or coincide with cubic reflections. Another possible explanation is the existence of sequences ...ABABAB... which are too thin to show well defined reflections from planes oblique to the hexagonal base plane. These sequences may be laterally disordered, which would explain the sawtooth profile of the hexagonal 100 peak. In this case the higher order hexagonal reflections would be weak (in agreement with the observation from the structure refinement of ice Ic, which indicates the absence of strong hexagonal peaks under the cubic lines). A clear distinction between these two options cannot be made at present, although the formation of complicated polytypes in a solid-solid recrystallization seems somewhat unlikely.

## Discussion

Ice Ic is found to be the cubic counterpart of ice Ih. Undoubtedly it is fully (or almost fully) disordered in its hydrogen arrangement with interatomic distances identical within the limit of error to ice Ih. The only significant structural difference is in the averaged  $O...O...O$  angles, which are perfectly tetrahedral (by symmetry) in ice Ic, while they are slightly different in ice Ih (according to the deviation from the ideal  $c/a$  ratio). The small particle size of ice Ic, the existence of deformation faults and some hexagonal component in the pattern obviously are inherent features of the material. Quantitative differences exist, e.g. for cubic ices prepared from different high pressure ices<sup>10</sup>, and can be readily explained by different amounts of hexagonal components exhibiting different degrees of disorder and/or different densities of deformation faults. It should be pointed out that the hexagonal components do not originate in ice Ih impurities, but should be understood as a component in the stacking sequence.

Ice Ic is generally assumed to be a metastable phase, although its natural occurrence seems to be established<sup>32</sup>. A transformation from ice Ih into ice Ic on cooling has never been observed; it either forms directly from the vapour or from some other solid ice phase. It has been observed repeatedly that very small crystallites of ice have a cubic habit<sup>33,34</sup> usually with dimensions  $< 1000$  Å. Moreover snow polycrystals very often show a misorientation of  $70.5-70.6^\circ$  between the  $c$ -axes<sup>35</sup>, which is equal to the angle between the 111 directions in cubic ice. It has been suggested<sup>35,36</sup> that ice nucleates preferentially with cubic symmetry, thus forming small crystallites of cubic habit. Multi-nucleation<sup>36</sup> may occur producing bulk cubic structures and hexagonal crystals (as the more stable phase)

will ultimately grow on the 111 faces of such a cubic (multi)nucleus, eventually forming hexagonal layers or twin crystals with the characteristic angle of  $70.53^\circ$ . It is conceivable that the change from a cubic to a hexagonal stacking is not abrupt, but happens over some distance, thus creating the stacking faults. Indeed, the analysis of the ice Ic powder pattern indicates the presence of both stacking faults and hexagonal sequences, the latter probably with some lateral disorder displacements. Apparently the initial stage of forming ice Ih is just reached when the recrystallization from amorphous or recovered high pressure ices ceases. The reorganization of their three-dimensionally hydrogen-bonded network of water molecules does not allow for the growth of the described twin crystals without heavily distorting the network at the twin boundary. This situation is different for crystal growth from the vapour, where the two twin domains could grow as columns without a twin boundary from the cubic nucleus as observed frequently in snow crystals<sup>35, 36</sup>. Branching of the crystal leaves unfilled space between the twin domains, which is hardly possible when a reorientation and reorganization of the hydrogen bonding takes place in the bulk. Thus the growth of ice Ih into the bulk may be inhibited by competing hexagonal layers on the cubic nucleus, which explains the absence of bulk ice Ih in the diffraction pattern as well as the lateral disorder within the hexagonal stacking sequences.

#### References

1. H. König, Z. Krist. 105 (1983) 279.
2. H.P. Barendrecht, Z. Phys. Chem. 20 (1896) 234.
3. J. Dewar, Chem. News 91 (1905) 216.
4. E.F. Burton & W.F. Oliver, Proc. Roy. Soc. London A153 (1936) 166.
5. R.L. McFarlan, Phys. Rev. 49 (1936) 644.
6. G. Honjo, N. Kitamura, K. Shimaoka & K. Mihama, J. Phys. Soc. Japan 11 (1956) 527.
7. L.G. Dowell & A.P. Rinfret, Nature 188 (1960) 1144.
8. J.E. Bertie, L.D. Calvert & E. Whalley, J. Chem. Phys. 38 (1963) 840.
9. J.E. Bertie, L.D. Calvert & E. Whalley, Can J. Chem. 42 (1964) 1373.
10. G.P. Arnold, E.D. Finch, S.W. Rabideau & R.G. Wenzel, J. Chem. Phys. 49 (1968) 4365.
11. A.J. Nozik & M. Kaplan, J. Chem. Phys. 47 (1967) 2960.
12. A. Elarby, J.F. Jal, J. Dupuy, P. Chieux, A. Wright & R. Parriens, J. Phys. Lett. 43 (1982) L355.
13. P.V. Hobbs, Ice Physics, Clarendon Press, Oxford, 1974.
14. R.H. Beaumont, H. Chihara & J.A. Morrison, J. Chem. Phys. 34 (1961) 1456.
15. J.A. McMillan & S.C. Los, Nature 206 (1965) 806.
16. J.A. Gormley, J. Chem. Phys. 48 (1968) 503.
17. C.A. Coulson & D. Eisenberg, Proc. Roy. Soc. London A291 (1966) 445.
18. W. Hagen, A.G.G.M. Tielens & J.M. Greenberg, Chem. Phys. 56 (1981) 367.
19. E.D. Finch, S.W. Rabideau & A.B. Denison, J. Chem. Phys. 49 (1968) 4660.
20. J.E. Berie & S.M. Jacobs, J. Chem. Phys. 67 (1977) 2445.
21. M. Blackman & N.D. Lisgarten, Proc. Roy. Soc. London A239 (1957) 93.
22. G. Honjo & K. Shimaoka, Acta Cryst. 10 (1957) 710.
23. F.V. Shallcross & G.B. Carpenter, J. Chem. Phys. 26 (1957) 782.
24. D.D. Klug & E. Whalley, J. Glaciol. 21 (1978) 782.
25. H. Gränicher, Z. Krist. 110 (1958) 432.
26. J. Paureau & C. Vettier, Rev. Sci. Instrum. 46 (1975) 1484.
27. U.H. Zucker, E. Perenthaler, W.F. Kuhs, R. Bachmann & H. Schulz, J. Appl. Cryst. 16 (1983) 358.
28. W.F. Kuhs & M.S. Lehmann, Water Science Reviews 2 (Ed. F. Franks) in press.
29. W.F. Kuhs & M.S. Lehmann, this conference.
30. T.R. Anantharaman & J.W. Christian, Acta Cryst. 9 (1956) 479.
31. M.S. Paterson, J. Appl. Phys. 23 (1952) 805.
32. E. Whalley, J. Phys. Chem. 87 (1983) 4174.
33. H. Fernandez-Moran, Ann. N.Y. Acad. Sci. 85 (1960) 689.
34. V.N. Vertsner & G.S. Zhdanov, Sov. Phys. Cryst. 10 (1966) 597.
35. T. Kobayashi, Y. Furukawa, T. Takahashi & H. Uyeda, J. Cryst. Growth 35 (1976) 262.
36. T. Takahashi & T. Kobayashi, J. Cryst. Growth 64 (1983) 593.